

Article

Analysis of Carbon Footprints and Surface Quality in Green Cutting Environments for the Milling of AZ31 Magnesium Alloy

Mohammad Kanan ^{1,*}, Sadaf Zahoor ², Muhammad Salman Habib ^{2,*}, Sana Ehsan ², Mudassar Rehman ³, Muhammad Shahzaib ², Sajawal Ali Khan ², Hassan Ali ², Zaher Abusaq ¹ and Allam Hamdan ⁴

¹ Jeddah College of Engineering, University of Business and Technology, Jeddah 21448, Saudi Arabia

² Department of Industrial and Manufacturing Engineering, University of Engineering and Technology, Lahore 39161, Pakistan; sadafzahoor@uet.edu.pk (S.Z.)

³ Department of Industry Engineering, School of Mechanical Engineering, Northwestern Polytechnical University, Xi'an 710072, China

⁴ Department of Accounting and Economics, College of Business and Finance, Ahlia University, Manama P.O. Box 10878, Bahrain

* Correspondence: m.kanan@ubt.edu.sa (M.K.); salmanhabib@uet.edu.pk (M.S.H.)

Abstract: This investigation delves into the effectiveness of employing vegetable-based cutting fluids and nanoparticles in milling AZ31 magnesium alloy, as part of the pursuit of ecologically sustainable manufacturing practices. The study scrutinizes three different cutting environments: (i) dry cutting; (ii) minimum quantity lubrication (MQL) with rice bran oil as the base oil and turmeric oil as an additive; and (iii) MQL with rice bran oil as the base oil, and turmeric oil and kaolinite nanoparticles as additives. Fuzzy logic was implemented to develop the design of experiments and assess the impact of these cutting environments on carbon emissions, surface quality, and microhardness. Upon conducting an analysis of variance (ANOVA), it was determined that all the three input parameters (cutting environment, cutting speed, and feed) greatly affect carbon emissions. The third cutting environment (MQL + bio-oils + kaolinite) generated the lowest carbon emissions (average of 9.21 ppm) and surface roughness value (0.3 μm). Confirmatory tests validated that the output parameters predicted using the multiobjective genetic algorithm aligned well with experimental values, thus affirming the algorithm's robustness.

Keywords: AZ31 magnesium alloy; vegetable oils; kaolinite nanoparticles; MQL; carbon emission; surface quality; genetic



Citation: Kanan, M.; Zahoor, S.; Habib, M.S.; Ehsan, S.; Rehman, M.; Shahzaib, M.; Khan, S.A.; Ali, H.; Abusaq, Z.; Hamdan, A. Analysis of Carbon Footprints and Surface Quality in Green Cutting Environments for the Milling of AZ31 Magnesium Alloy. *Sustainability* **2023**, *15*, 6301. <https://doi.org/10.3390/su15076301>

Academic Editors: Sikiru Oluwarotimi Ismail, Azwan Iskandar Azmi, Norshah Aizat Shuaib and Muhamad Nasir Murad

Received: 22 February 2023

Revised: 3 April 2023

Accepted: 5 April 2023

Published: 6 April 2023



Copyright: © 2023 by the authors. Licensee MDPI, Basel, Switzerland. This article is an open access article distributed under the terms and conditions of the Creative Commons Attribution (CC BY) license (<https://creativecommons.org/licenses/by/4.0/>).

1. Introduction

Humanity is currently facing a substantial obstacle to achieving sustainable growth due to the rapid expansion of industries and the rising cost of resources. This, in turn, has resulted in an increase in carbon emissions, which poses a significant threat to the environment and exacerbates the challenges to achieving sustainable development [1]. Carbon emissions are a significant contributor to climate change, with the burning of fossil fuels being the primary source of these emissions that also serves as the power source for industry. The release of carbon dioxide and other greenhouse gases into the atmosphere traps heat and causes global warming, resulting in a range of impacts such as sea level rise, more frequent and severe weather events, and changes to ecosystems and wildlife [2]. In addition, carbon emissions can have health impacts on humans, particularly in areas with high levels of air pollution. The need to reduce carbon emissions and transition to more sustainable energy sources is crucial to mitigating these impacts and limiting the severity of climate change [3,4].

In the manufacturing industry, metal cutting operations are recognized as the prime contributor to carbon emissions, with power consumption, cutting fluid, tool material, and

workpiece material being the main sources of emissions. Machining processes, such as milling and turning, are considered the most energy-intensive processes; they account for a significant proportion of the total power consumption, with their energy usage making up 75% of the total energy consumption in manufacturing. In numerical control machining operations, unit energy consumption ranges from 66 to 82 MJ/kg [5,6], further emphasizing the importance of energy conservation and emission reduction in this area. According to IEA studies, the manufacturing sector is responsible for about one-third of the usage of global energy and causes about 36% of global carbon emissions [1]. Furthermore, the annual emissions of CO₂ and SO₂ from a CNC machine tool with a spindle power of 22 kW are comparable with the electricity consumption of 61 automobiles and 248 sport utility vehicles [7]. Cutting fluids, which are utilized to cool and lubricate the cutting tool during machining, can generate a significant amount of carbon emissions through the use of synthetic or petroleum-based oils. Additionally, tool materials such as carbide and diamond can result in carbon emissions during their production, which can contribute to the overall carbon footprint of the machining process. Finally, workpiece materials such as steel, aluminum, and titanium can produce carbon emissions during production and processing. It is evident that undertaking research on the resource consumption, energy conservation, and emissions reduction for metal cutting processes is of paramount importance and ecological urgency.

One potential solution to address these issues is to eliminate the use of cutting fluids during machining, which is commonly known as dry machining. While dry machining is often viewed as an environmentally friendly option, it can lead to significant challenges due to the high friction between the tool and workpiece in the absence of lubrication during cutting. This can result in excessive heat generation, increased cutting forces, reduced tool lifespan, and a low-quality surface finish on the workpiece [8–10]. Consequently, using a lubrication method is crucial in the machining process as it provides necessary cooling, lubrication, and removal of chip debris from the tool–chip contact. Wet machining is often preferred for difficult-to-machine materials and high-speed cutting approaches due to the high temperatures and cutting forces generated during the process [11]. Proper cutting fluids can help mitigate these challenges and achieve a better surface quality of the machined parts [12,13]. However, the commonly used low-cost mineral oils, which are nonbiodegradable, have better friction-reducing characteristics. They account for about 16% of total manufacturing costs and may increase to 30% when working with difficult-to-handle alloys [14]. Additionally, disposing of these fluids incurs high costs due to their nonbiodegradable composition and labor-intensive pre-disposal treatment, which can be up to four times the acquisition cost in the United States and Europe [15]. High disposal costs are a result of the cutting fluids' nonbiodegradable composition and the labor-intensive pre-disposal treatment. Various environmental organizations worldwide have imposed strict regulations on the disposal of used cutting fluids [16,17].

The use of mineral oil-based cutting fluids can have a negative impact on the environment and human health, as they can release harmful pollutants, such as volatile organic compounds (VOCs) and particulate matter, which can affect air quality. Furthermore, the combustion of mineral oil during machining can release substantial amounts of carbon dioxide and other greenhouse gases, which contribute to global warming. The presence of bacteria in cutting fluids is an additional concern as it may affect various aspects of the machining process, including emulsion stability, lubrication, pH content, corrosion inhibition, and human health [18,19]. The use of chemical additives to prevent bacterial growth is often necessary, but it can delay or hinder the natural degradation of cutting fluids [20]. Exposure to toxic mineral oils is linked to an increased risk of skin cancer in the workplace, underscoring the need to reduce the use of mineral oil in machining and explore more sustainable lubricants. As cutting fluids pose environmental and health risks, researchers explore methods to reduce their use, such as the minimum quantity lubrication technique (MQL). Garcia and Ribeiro [21] discovered a 50% improvement in tool life using MQL compared to dry end milling of Ti-6Al-4V alloys. Working on MQL, Liu et al. [22]

concluded that air pressure and nozzle location has a direct effect on cutting force and cutting temperature. Similarly, Werda et al. [23] discovered that synthetic ester oil-assisted MQL is effective for the machined surface integrity.

To address the limitations of conventional cutting fluids, vegetable oils have been developed as an alternative due to their excellent lubrication qualities and ability to perform well in low temperatures [24]. However, vegetable oils are also prone to poor oxidation stability. Several studies have been conducted to investigate the use of vegetable oils as base fluids for industrial lubricants, including sunflower oil [25,26], coconut oil [27], rice bran oil [28], and jatropha oil [29]. Research carried out by Gonzaga et al. [30] shows that rice bran oil exhibits better stability compared to other vegetable oils, such as canola, sunflower, soybean, cottonseed, and maize oils. Rani et al. [31] discovered that rice bran oil contains natural antioxidants, which makes it less susceptible to wear than other vegetable oils. Rice bran oil's high oleic acid content (38.4 percent) increases its oxidation stability, and it has demonstrated superior properties in thermal, oxidative, physical, and tribological tests when compared to other oils [32]. Various methods, such as epoxidation, additions, and esterification, have been employed to enhance the properties of vegetable oils [33]. Turmeric, known for its anti-inflammatory properties due to its curcuminoids, flavonoids, and phenolic contents, is often used as a natural antioxidant. In this study, turmeric oil was utilized as a natural antioxidant additive to improve the performance of rice bran oil.

The discovery of nanopowders has revolutionized a vast array of industries. In the field of tribology, nanoparticles such as ZnO and CuO have been added to vegetable oils such as soybean and coconut to improve their performance [34–36]. Recently, halloysite nanotubes and kaolinite clay nanopowder have been incorporated into biodegradable cutting fluids. Halloysite and kaolinite are both hydrated aluminum silicates with dioctahedral 1:1 layer structures, although halloysite contains more water contents [37–40]. These nanoparticles are commonly found in a spheroidal shape, although they can also exhibit tubular or platy forms [41]. Recently, kaolinite has been identified as having the remarkable ability to sequester carbon dioxide (CO₂) from the atmosphere. By incorporating kaolinite into cutting fluids during machining, it may serve as a sustainable and ecofriendly solution for mitigating CO₂ emissions in the manufacturing sector. Kaolinite's CO₂-absorption capacity is attributable to its large surface area and unique crystal structure, which enables it to capture and retain CO₂ molecules. Kaolinite was chosen as a substitute for halloysite in this study due to its wider availability and lower cost [42,43].

The above-cited literature highlights a significant research void concerning the viability of utilizing bio-oils and kaolinite as potential solutions to curb carbon emissions in the machining industry, as well as to better machining characteristics. This gap in knowledge necessitates further investigation into the efficacy of these sustainable alternatives to cutting fluids, particularly their tribological characteristics and carbon capture capabilities. This study could shed light on the potential of using these materials as ecofriendly alternatives to traditional cutting fluids, leading to a significant reduction in carbon footprint and machining gain in the manufacturing industry. In this study, three cutting environments, namely (i) dry cutting, (ii) minimum quantity lubrication (MQL) with rice bran oil as the base oil and turmeric oil as an additive, and (iii) MQL with rice bran oil as the base oil and turmeric oil and kaolinite (nanoparticles) as additives, were investigated for milling of AZ31 magnesium alloy. Fuzzy logic was utilized to develop the design of the experiments. This research aims to evaluate the impact of kaolinite and bio-oils on the carbon footprint and machining performance of the cutting process in terms of surface roughness (SR) and microhardness (HV). The two machining responses are considered from the perspective of achieving better osteointegration characteristics of implants, as the selected workpiece material AZ31 magnesium alloy is widely used for bioimplant applications.

Section 2 of the paper shall elaborate on the intricate details of the materials and methods used in this study. Following this, Section 3 shall delve into an extensive analysis of the results and an insightful discussion. Finally, the paper shall culminate with Section 4, where conclusions will be drawn and recommendations for future research shall be presented.

2. Materials and Methods

Sustainability in machining involves a holistic approach that considers the environmental impact of all aspects of the machining process, from material selection to cutting environment, and from disposal of cutting fluids to minimizing of carbon emissions. Therefore, a conscious selection of AZ31 magnesium alloy as the workpiece material during this study was made due to its desirable properties such as strength-to-weight ratios, stiffness/stability ratios, biodegradability, and low environmental impact [44,45]. The alloy is commonly used in industries such as the automotive and aerospace industries, though it has become a favorable choice for bioimplant applications due to its similar mechanical properties to human bone. Compared to other commonly used bioimplant metals such as titanium alloys and stainless steel (4.47 g/cm³ and 7.8 g/cm³, respectively), magnesium alloys have lower densities, ranging from 1.7 to 1.9 g/cm³ [46]. The chemical composition of the AZ31 alloy can be found in Table 1, obtained from X-ray diffraction (XRD) method using X-ray diffractometer (EQUINOX 2000, Inel Inc., Stratham, NH, USA) with Co K α source at a 111° diffraction angle, and Table 2 provides information on its mechanical and thermal properties. To conduct the experiments, a rectangular plate of the alloy measuring 160 mm \times 60 mm \times 16 mm was prepared for end milling of a slot (60 mm \times 4 mm \times 3 mm) using a CNC machining center (MCV 600, Long Chang Mechanical Industrial Co., Ltd., Taipei, Taiwan) [9,10]. During the cutting process, a four-flute end mill cutter with a 4 mm diameter, coated with titanium aluminum nitride (TiAlN), was used, and a new cutter was used for each experiment condition.

Table 1. Chemical composition of AZ31 magnesium alloy.

| Element | Mg | Al | Zinc, Zn | Mn | Si | Cu | Ca | Fe | Ni |
|---------|-----|-------|----------|-------|-------|--------|--------|---------|---------|
| Wt.% | 97% | 2.50% | 0.60% | 0.20% | 0.10% | 0.050% | 0.040% | 0.0050% | 0.0050% |

Table 2. Mechanical and thermal properties of AZ31.

| Property | Value |
|----------------------------------|-------|
| Density (g/cm ³) | 1.78 |
| Compressive yield strength (MPa) | 60–70 |
| Ultimate tensile strength (MPa) | 235 |
| Flash point (°C) | 628 |
| Elastic modulus (MPa) | 45 |
| Thermal conductivity (W/m °C) | 96 |

The experiments in this study were conducted using the robust fuzzy logic DOE technique [47]. After conducting a thorough literature review [9,10,48] and preliminary experimentation, three control variables were chosen at three levels, namely the cutting environment, the cutting speed (CS), and the feed (F), as presented in Table 3. Given the bio-compatibility of AZ31, the study focused on two machining responses, surface roughness (SR) and microhardness (HV), while taking into account carbon footprints as prime response parameter. To analyze the carbon footprint, milling was performed on magnesium alloy AZ31 under three different cutting environments: (i) dry machining, (ii) minimum quantity lubrication (MQL) using rice bran oil as the base oil and turmeric oil as an additive, and (iii) MQL using rice bran oil as the base oil and turmeric oil and kaolinite (nanoparticles) as additives. The internal mixed MQL method with a flow rate of 25 mL/h, 45° nozzle angle, and 30 mm standoff distance was used, with a nozzle internal diameter of 1.78 mm.

Table 3. Details of control and constant variables.

| Level | Control Variable | | Constant Variable | | | | |
|-------|--|-----------------------------|-------------------|------------------------------|-------------------------------|----------------|------------------|
| | Cutting Environment | Cutting Speed (CS) (mm/min) | Feed (F) (mm/min) | Axial Depth of Cut (Ap) (mm) | Radial Depth of Cut (Ar) (mm) | Tool Hang (mm) | Number of Flutes |
| 1 | Dry | 40 | 70 | 0.15 | 4 | 32 | 4 |
| 2 | MQL) with rice bran oil and turmeric oil | 48 | 80 | | | | |
| 3 | MQL with rice bran oil, turmeric oil and kaolinite | 56 | 90 | | | | |

For the cutting fluid preparation, the magnetic stirrer (CJJ78-1, Jiangsu Jinyi Instrument Technology Co., Ltd., Changzhou, China) was used to mix the rice bran oil, the turmeric oil, and the kaolinite with the 10 min stirring time. The properties of the oils and nanopowder used in the minimum quantity lubrication (MQL) cutting environment are shown in Table 4, while Figure 1a depicts the specifications of the three cutting environments employed in the experimental research.

Table 4. Prosperities of bio-oils used as cutting fluid.

| Property | Rice Bran Oil | Turmeric Oil | Kaolinite (Al ₂ Si ₂ O ₅ (OH) ₄) |
|----------------------|---------------|--------------|---|
| Viscosity (Pa.s) | 0.0398 | high | - |
| Flash point (°C) | 232 | 99 | - |
| Lubricity | high | high | - |
| Oxidation stability | high | high | - |
| Environmental impact | high | high | high |

To measure carbon emissions during machining, a CO and CO₂ meter (Testo 315-3, Testo SE & Co., Titisee-Neustadt, Germany) was used. The meter was placed inside the machining chamber (see Figure 1b) to ensure that only carbon emissions from the machining process were measured, excluding those from the external environment. The meter is designed for parallel measurement of CO and CO₂ in ambient air and is compliant with European standard EN 50543 [49]. In addition, the CNC machining center used for the experimentation was operated exclusively within the laboratory to prevent contamination from external carbon emissions. The surface roughness of each slot was measured in terms of Ra using a surface texture meter (Surtronic S128, Taylor Hobson, Leicester, UK) with a 4 mm evaluation length and 0.8 mm cutoff length. Three readings were taken across the length of the slot (i.e., start, center, and end of the slot), and the average value is presented in this subsequent section.

The microhardness of the machined samples was measured using a microhardness tester (HMV2, Shimadzu Corporation, Kyoto, Japan). The samples were cut from the end of the milled slot using a wire-cut electric discharge machine because this position was expected to exhibit a more aggressive effect of tool wear. The microhardness values were measured perpendicular to the machined surface in the feed direction using 25 g of test force and 10 s of measuring time. Four indentations were made, with the first three points spaced 50 µm apart and the fourth point located 250 µm from the machined surface. To determine the significant input factors, a parametric effect analysis and an analysis of variance (ANOVA) were conducted at a 95% confidence level using MiniTab 2021. Given that higher microhardness is desirable for bioimplant applications to enhance

wear resistance, and lower surface finish is needed for corrosion resistance, a genetic algorithm (GA) technique was utilized to optimize these outputs using R2022b MATLAB.

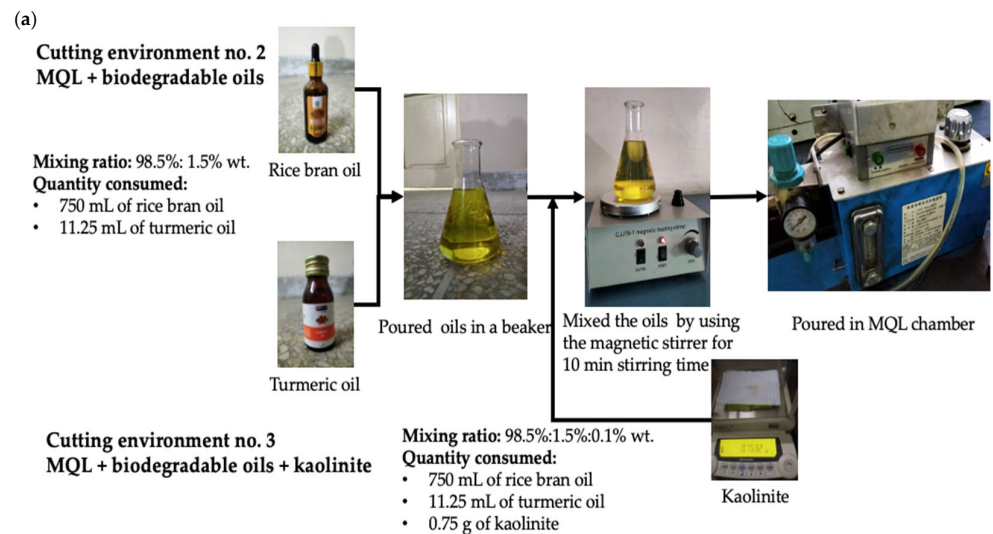


Figure 1. Experimental details, (a) cutting environment details; (b) experimental setup.

3. Results

To compare the carbon emissions and machining characteristics of AZ31 under different cutting environments, three sets of experiments were conducted with 27 test runs of slot milling. The experiments were replicated to ensure the accuracy and consistency of the results. The measurements of carbon emissions, surface roughness, and microhardness were taken carefully, and the results were recorded in Table 5.

3.1. Carbon Footprint

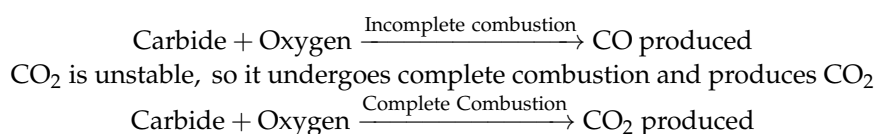
Measuring the carbon footprint of milling operations is essential for identifying sources of greenhouse gas emissions and evaluating the effectiveness of emission reduction strategies. The quantitative results of carbon emissions, obtained using the fuzzy logic technique, are presented in Table 5. To analyze the effects of different parameters on the carbon footprint, main effects plots were generated and depicted in Figure 2. The results show that the cutting environment has a decreasing linear trend on carbon emissions, while cutting speed (CS) and feed (F) exhibit increasing linear behavior. Furthermore, the carbon footprint

was observed to decrease under the third cutting environment, which involved the use of MQL with rice bran base oil, turmeric oil, and kaolinite nanoparticles as additives. Table 5 and Figure 2 demonstrate that the minimum carbon emission (−29.2 ppm) was achieved with the use of MQL with rice bran base oil, turmeric oil, and kaolinite nanoparticles as additives at 40 m/min cutting speed (CS), while the highest carbon value (109 ppm) was observed in a dry environment at the same cutting speed.

Table 5. Experimental results after milling of AZ31 magnesium alloy using fuzzy logic DOE technique.

| Exp. No. | Control Parameter | | | Response Parameter | | |
|----------|--|-----------------------------|-------------------|----------------------------|-----------------------------|---|
| | Cutting Environment | Cutting Speed (CS) (mm/min) | Feed (F) (mm/min) | Carbon Emission (CE) (ppm) | Surface Roughness (SR) (um) | Microhardness Perpendicular at 50 um (HV) |
| 1 | Dry cutting | 40 | 70 | 109 | 0.7 | 80 |
| 2 | | 40 | 80 | 85 | 0.9 | 72 |
| 3 | | 40 | 90 | 1.83 | 0.6 | 63 |
| 4 | | 48 | 70 | 9.33 | 0.6 | 52 |
| 5 | | 48 | 80 | 33.66 | 0.6 | 76 |
| 6 | | 48 | 90 | 21.33 | 0.7 | 83 |
| 7 | | 56 | 70 | 24.83 | 0.6 | 82 |
| 8 | | 56 | 80 | 1.33 | 0.4 | 66 |
| 9 | | 56 | 90 | 8.83 | 0.6 | 72 |
| 10 | MQL + rice bran oil and turmeric oil | 40 | 70 | 34 | 0.8 | 82 |
| 11 | | 40 | 80 | 13 | 0.4 | 82 |
| 12 | | 40 | 90 | 6 | 0.5 | 82 |
| 13 | | 48 | 70 | 43 | 0.5 | 70 |
| 14 | | 48 | 80 | 34 | 0.5 | 92 |
| 15 | | 48 | 90 | 41 | 0.6 | 80 |
| 16 | | 56 | 70 | 15 | 0.4 | 84 |
| 17 | | 56 | 80 | 26 | 0.6 | 56 |
| 18 | | 56 | 90 | 20 | 0.4 | 60 |
| 19 | MQL + rice bran oil and turmeric oil + kaolinite | 40 | 70 | 30 | 0.6 | 71 |
| 20 | | 40 | 80 | 9 | 0.5 | 81 |
| 21 | | 40 | 90 | −29.2 | 0.6 | 65 |
| 22 | | 48 | 70 | 0.5 | 0.6 | 65 |
| 23 | | 48 | 80 | 30.2 | 0.5 | 65 |
| 24 | | 48 | 90 | 8.5 | 0.5 | 67 |
| 25 | | 56 | 70 | 7.52 | 0.6 | 65 |
| 26 | | 56 | 80 | 4.33 | 0.4 | 67 |
| 27 | | 56 | 90 | 22 | 0.3 | 57 |

The analysis of carbon footprints conducted during this study indicates that the friction generated during the vertical milling of AZ31 magnesium alloy, when the carbide end mill cutter comes in direct contact with the workpiece, results in the production of heat [50–52]. This heat causes oxidation of the carbide in the TiAlN-coated carbide end mill cutter, leading to the release of CO and CO₂ due to the presence of oxygen in the atmospheric air.



In addition, carbon emissions during machining were also attributed to the surrounding air. The atmospheric air contains 417 ppm of carbon dioxide due to global warming and climate change. In this study, under dry cutting conditions, the primary source of carbon

emission was found to be the tool material, i.e., carbide. In the MQL cutting environment, rice bran oil and turmeric oil were used as cutting fluids. These oils contain fatty acids and unsaturated double bonds, but they generate less CO₂ during the metal cutting process compared to mineral oil and kerosene oil, mainly because of their higher volatile temperature values. Rice bran and turmeric oils have volatile temperatures of 232 °C and 183 °C, respectively, while mineral oil and kerosene oil have volatile temperatures of 168.3 °C and 38 °C, respectively [28]. It is believed that the vegetable oils prevent the TiAlN coating of the carbide end mill cutter from damage and also reduce the heat generation, resulting in fewer emissions being produced, as shown in Table 6.

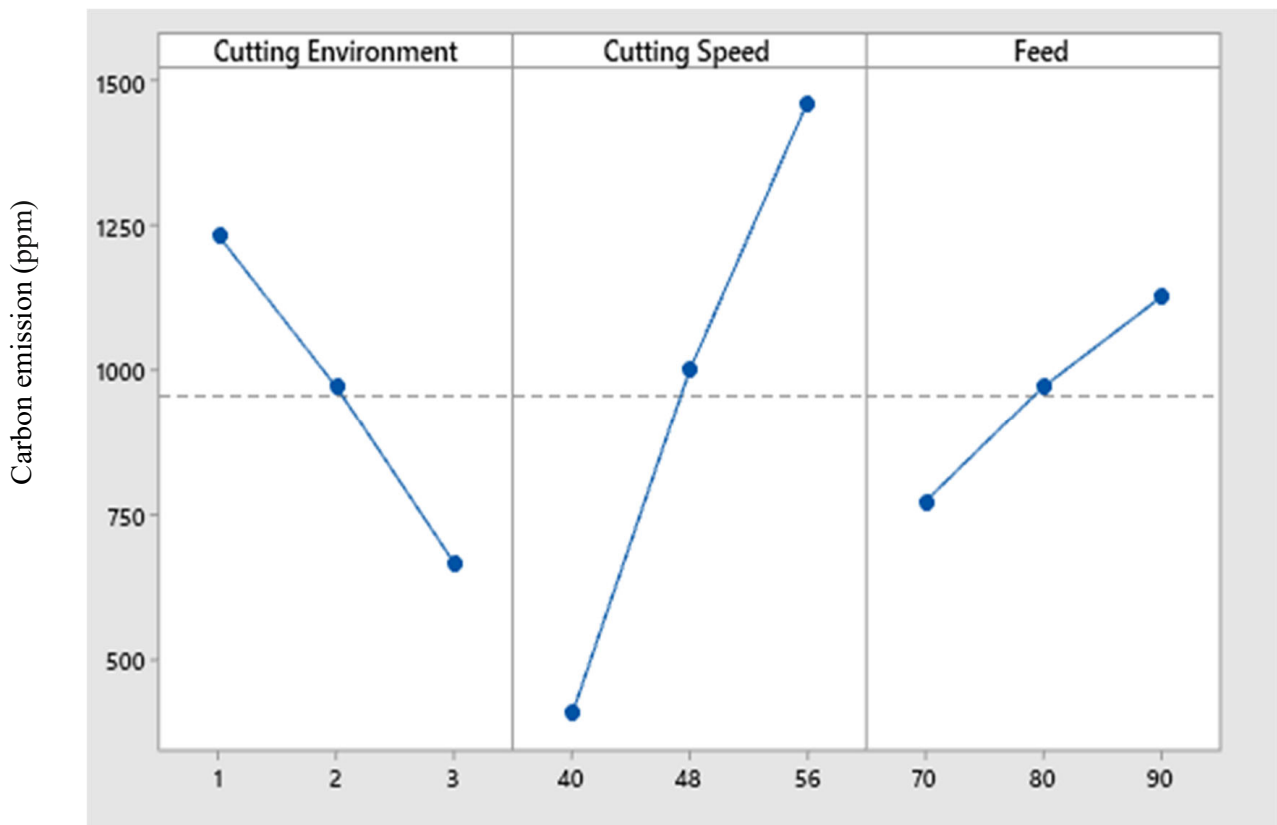


Figure 2. Main effect plots of carbon emission.

Table 6. Comparison of carbon emission among three cutting environments used in the present study.

| Cutting Environment | Average CO ₂ Production(ppm) | CO ₂ Production with Reference to Dry Machining (%) | CO ₂ Reduction (%) |
|----------------------------|---|--|-------------------------------|
| Dry machining | 32.79 | 100 | 100 |
| MQL + bio oils | 23.88 | 72.8 | 27.2 |
| MQL + bio oils + kaolinite | 9.20 | 28 | 72 |

To further analyze the effects of process parameters on carbon emissions of AZ31, a quantitative analysis of the process parameters was conducted using ANOVA with a confidence interval of 95% ($\alpha = 5\%$). The results are presented in Table 7, which shows that the three control variables, cutting environment, CS, and feed (F), are significant with a “*p* value” less than 0.05 and contribute 19.39%, 66.9%, and 7.5%, respectively.

Table 7. ANOVA analysis of carbon emission at 95% confidence interval.

| Source | DF | Adj SS | Adj MS | F-Value | p-Value | Contribution |
|---|----|-----------|-----------|---------|---------|--------------|
| Model | 9 | 7,089,249 | 787,694 | 39.00 | 0.000 | |
| Linear | 3 | 6,980,654 | 2,326,885 | 115.20 | 0.000 | |
| Cutting environment | 1 | 1,441,590 | 1,441,590 | 71.37 | 0.000 | 19.39% |
| Cutting speed | 1 | 4,974,499 | 4,974,499 | 246.28 | 0.000 | 66.9% |
| Feed | 1 | 564,565 | 564,565 | 27.95 | 0.000 | 7.5% |
| Square | 3 | 31,888 | 10,629 | 0.53 | 0.670 | |
| Cutting environment × cutting environment | 1 | 2868 | 2868 | 0.14 | 0.711 | |
| Cutting speed × cutting speed | 1 | 26,093 | 26,093 | 1.29 | 0.271 | |
| Feed × feed | 1 | 2926 | 2926 | 0.14 | 0.708 | |
| 2-way interaction | 3 | 76,707 | 25,569 | 1.27 | 0.318 | |
| Cutting environment × cutting speed | 1 | 62,267 | 62,267 | 3.08 | 0.097 | |
| Cutting environment × feed | 1 | 5078 | 5078 | 0.25 | 0.623 | |
| Cutting speed × feed | 1 | 9362 | 9362 | 0.46 | 0.505 | |
| Error | 17 | 343,376 | 20,199 | | | |

3.2. Surface Roughness

Ensuring the surface quality of machined parts is crucial for their performance, and it can be measured both quantitatively and qualitatively. The quantitative results of average surface roughness (SR) obtained using the fuzzy logic technique are presented in Table 5. To analyze the effects of different parameters on SR, main effects plots were generated, depicted in Figure 3. The results show that cutting environment and cutting speed exhibit a decreasing linear trend on SR, while feed (F) demonstrates a nonlinear behavior. Additionally, the surface finish was found to be improved under the third cutting environment, which involved the use of MQL with rice bran base oil, and turmeric oil and kaolinite nanoparticles as additives. Table 5 and Figure 3 demonstrate that the minimum surface roughness (0.3 μm) was obtained using MQL with rice bran base oil and turmeric oil and kaolinite nanoparticle additives at 56 m/min cutting speed (CS), while the highest SR value (0.9 μm) was observed in a dry environment at 40 m/min CS.

When it comes to surface roughness, the combination of MQL with biodegradable vegetable oils and kaolinite nanoparticles as a cutting fluid has shown to have excellent cooling and lubricating properties, leading to improved surface quality. Machining of AZ31 magnesium alloy is known to be hazardous due to its flammability during heat generation in the shear zone, but this issue has been addressed with the use of turmeric oil as an additive, which has antioxidant properties. Furthermore, it is widely acknowledged that friction occurring at the tool–workpiece interface is a major factor negatively affecting the surface quality of machined parts [53]. In addition, the literature suggests that high surface roughness values are associated with small cutting speeds and high feed rates [54]. Specifically, poor surface quality at low cutting speeds is attributed to the high tensile stresses generated by friction, while the presence of uncut metal is reported to cause high surface roughness values at high feed rates due to the increased distance between two successive tool runs [55]. The results of this study are consistent with the aforementioned literature.

Machining with vegetable oils offers numerous advantages, mainly due to the presence of fatty acids that create a strong lubrication film between the tool and workpiece. This reduces friction and enhances antiwear properties due to the polar nature of the fatty acids. The resulting oiliness contributes to improved surface integrity of the machined component. Furthermore, vegetable-based cutting fluids have higher flash points than mineral oils,

which reduces the risk of smoke formation and fire hazards during the machining process of AZ31 alloy.

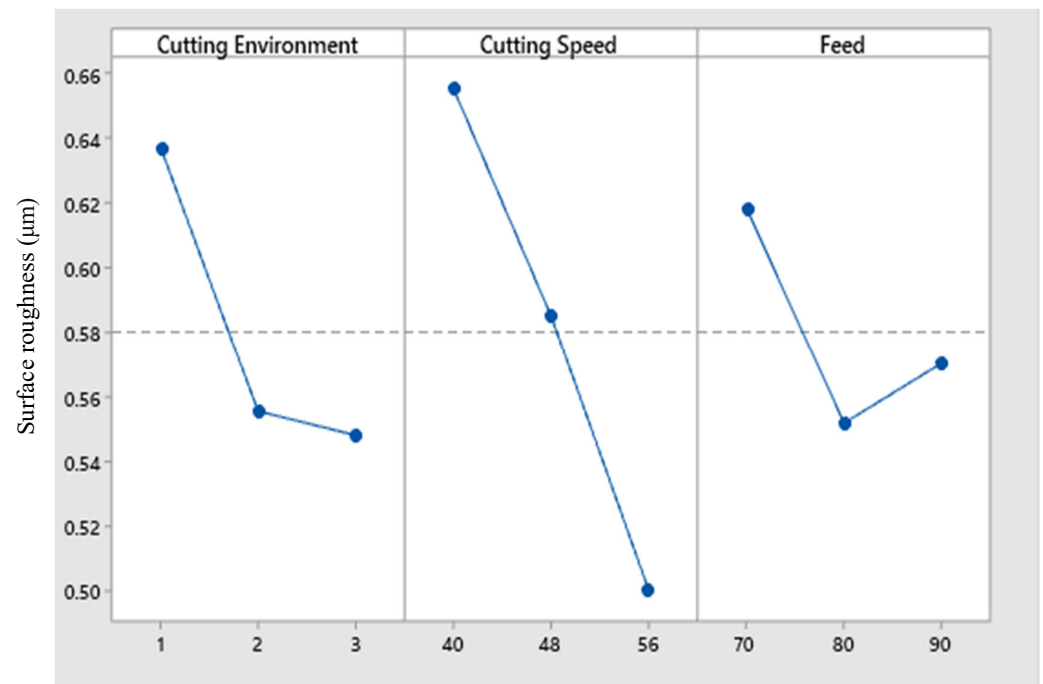


Figure 3. Main effect plots of surface roughness.

After analyzing the effects of process parameters on SR of AZ31, a quantitative analysis of the process parameters was conducted using ANOVA with a confidence interval of 95% ($\alpha = 5\%$), and the results are presented in Table 8. The cutting speed was found to be significant with a “*p* value” less than 0.05 and contributed 30.10%.

Table 8. ANOVA analysis of surface roughness at 95% confidence interval.

| Source | DF | Adj SS | Adj MS | F-Value | <i>p</i> -Value | Contribution |
|---|----|----------|----------|---------|-----------------|--------------|
| Model | 9 | 0.189506 | 0.021056 | 2.09 | 0.091 | |
| Linear | 3 | 0.154877 | 0.051626 | 5.13 | 0.010 | |
| Cutting environment | 1 | 0.035556 | 0.035556 | 3.53 | 0.077 | 9.8% |
| Cutting speed | 1 | 0.108889 | 0.108889 | 10.82 | 0.004 | 30.10% |
| Feed | 1 | 0.010432 | 0.010432 | 1.04 | 0.323 | 2.8% |
| Square | 3 | 0.019444 | 0.006481 | 0.64 | 0.597 | |
| Cutting environment × cutting environment | 1 | 0.008230 | 0.008230 | 0.82 | 0.378 | |
| Cutting speed × cutting speed | 1 | 0.000329 | 0.000329 | 0.03 | 0.859 | |
| Feed × feed | 1 | 0.010885 | 0.010885 | 1.08 | 0.313 | |
| 2-way interaction | 3 | 0.015185 | 0.005062 | 0.50 | 0.685 | |
| Cutting environment × cutting speed | 1 | 0.003333 | 0.003333 | 0.33 | 0.572 | |
| Cutting environment × feed | 1 | 0.005926 | 0.005926 | 0.59 | 0.453 | |
| Cutting speed × feed | 1 | 0.005926 | 0.005926 | 0.59 | 0.453 | |
| Error | 17 | 0.171070 | 0.010063 | | | |

3.3. Microhardness (Perpendicular to the Machining Surface at Distance of 50 μm)

Table 5 presents the results of microhardness measurements taken perpendicular to the machining direction for all test runs under three cutting environments. Four points were recorded with a 50 μm interval starting from 50 μm depth beneath the machined surface. The microhardness values showed an increase under a depth of 50 μm compared to the bulk hardness (72 HV) in the second cutting environment (MQL with rice bran and turmeric oil). To analyze the effects of process parameters on microhardness, main effects plots were drawn, presented in Figure 4. As seen from the figure, the cutting environment and feed exhibit a nonlinear trend, while the cutting speed shows a decreasing linear behavior. The microhardness of the milled samples was measured perpendicular to the machining direction in all three cutting environments. Four measurement points were taken with a 50 μm interval, starting from a depth of 50 μm beneath the machined surface. Table 5 provides the quantitative results of microhardness obtained through fuzzy logic technique.

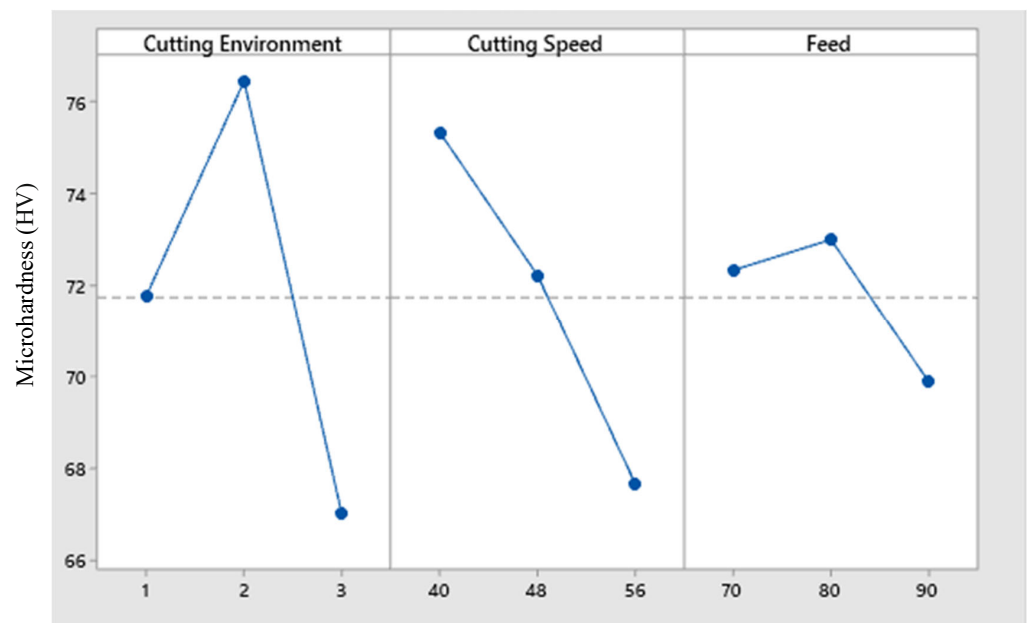


Figure 4. Main effect plots of microhardness.

The second cutting environment, which involved MQL with rice bran and turmeric oil, showed an increase in microhardness values below 50 μm depth compared to the bulk hardness (72 HV). To analyze the effects of process parameters on microhardness, main effects plots were generated, shown in Figure 4. From Figure 4, it can be observed that the cutting environment and feed exhibit a nonlinear trend, while the cutting speed shows a decreasing linear behavior. Regarding cutting methods, the highest microhardness value (84 HV) was obtained with the use of MQL with rice bran base oil and turmeric oil at a cutting speed of 56 m/min, as shown in Table 5 and Figure 4.

The microhardness of the machined surface and subsurface is typically affected by the heat generated during the machining process [56,57]. This is due to the fact that workpiece materials with high thermal conductivity tend to absorb the generated heat, resulting in plastic deformation and the reorientation of grain boundaries. Such a phenomenon can significantly alter the mechanical properties of the component and ultimately impact the machinability of alloys.

Moreover, inadequate or ineffective cooling methods in the absence of coolant fail to dissipate the heat generated in the cutting zone, resulting in severe tool wear. This, in turn, leads to increased strain hardening and plastic deformation in the subsurface layers. On the other hand, the combination of vegetable oil and kaolinite nanoparticles used in this

study exhibited excellent lubrication and cooling properties, effectively dissipating heat from the shear zone, thus minimizing work hardening.

After performing parametric effect analysis for microhardness of AZ31, quantitative analysis of process parameters was carried out using ANOVA at 95% confidence interval ($\alpha = 5\%$), as presented in Table 9. It can be seen that all three control variables are insignificant with a “ p value” greater than 0.05. However, the cutting environment and cutting speed are the most contributing factors, with 9.8% and 3.8% contribution, respectively.

Table 9. ANOVA analysis of microhardness at 95% confidence interval.

| Source | DF | Adj SS | Adj MS | F-Value | p -Value | Contribution |
|--|----|---------|---------|---------|------------|--------------|
| Model | 9 | 859.50 | 95.500 | 0.89 | 0.553 | |
| Linear | 3 | 394.11 | 131.370 | 1.23 | 0.331 | |
| Cutting environment | 1 | 102.72 | 102.722 | 0.96 | 0.341 | 3.8% |
| Cutting speed | 1 | 264.50 | 264.500 | 2.47 | 0.135 | 9.8% |
| Feed | 1 | 26.89 | 26.889 | 0.25 | 0.623 | 1% |
| Square | 3 | 323.22 | 107.741 | 1.01 | 0.414 | 12% |
| Cutting environment \times cutting speed | 1 | 298.69 | 298.685 | 2.79 | 0.113 | 11% |
| Cutting speed \times cutting speed | 1 | 3.13 | 3.130 | 0.03 | 0.866 | 0.1% |
| Feed \times feed | 1 | 21.41 | 21.407 | 0.20 | 0.661 | 0.7% |
| 2-way interaction | 3 | 142.17 | 47.389 | 0.44 | 0.726 | 5% |
| Cutting environment \times cutting speed | 1 | 90.75 | 90.750 | 0.85 | 0.370 | 3.3% |
| Cutting environment \times feed | 1 | 21.33 | 21.333 | 0.20 | 0.661 | 0.7% |
| Cutting speed \times feed | 1 | 30.08 | 30.083 | 0.28 | 0.603 | 1.1% |
| Error | 17 | 1821.69 | 107.158 | | | |

3.4. Empirical Modelling

Regression analysis was utilized to create empirical models for the response attributes (carbon emission, cutting speed, and feed), which are represented by Equations (1)–(3).

$$\text{Carbon emission} = -9386 + 401 \times \text{CE} + 210.6 \times \text{CS} + 73.9 \times \text{F} - 21.9 \times \text{CE} \times \text{CE} - 1.030 \times \text{CS} \times \text{CS} - 0.221 \times \text{F} \times \text{F} - 9.00 \times \text{CE} \times \text{CS} - 2.06 \times \text{CE} \times \text{F} - 0.349 \times \text{CS} \times \text{F} \quad (1)$$

$$\text{Surface roughness} = 4.80 - 0.115 \times \text{CE} - 0.0250 \times \text{CS} - 0.0794 \times \text{F} + 0.0370 \times \text{CS} \times \text{CS} - 0.000116 \times \text{CS} \times \text{CS} + 0.000426 \times \text{F} \times \text{F} + 0.00208 \times \text{CE} \times \text{CS} - 0.00222 \times \text{CE} \times \text{F} + 0.000278 \times \text{CS} \times \text{F} \quad (2)$$

$$\text{Microhardness} = -190 + 53.0 \times \text{CE} + 2.88 \times \text{CS} + 4.12 \times \text{F} - 7.06 \times \text{CE} \times \text{CE} - 0.0113 \times \text{CS} \times \text{CS} - 0.0189 \times \text{F} \times \text{F} - 0.344 \times \text{CE} \times \text{CS} - 0.133 \times \text{CE} \times \text{F} - 0.0198 \times \text{CS} \times \text{F} \quad (3)$$

Upon graphically plotting the difference between the experimental and predicted values (obtained through regression analysis) using Equations (1)–(3), it was observed that the difference between the actual and predicted values was less than 20% data error, indicating the reliability of the empirical models. This is depicted in Figure 5a–c, which show the percentage error between the experimental and predicted values for carbon emission, surface roughness, and microhardness, respectively.

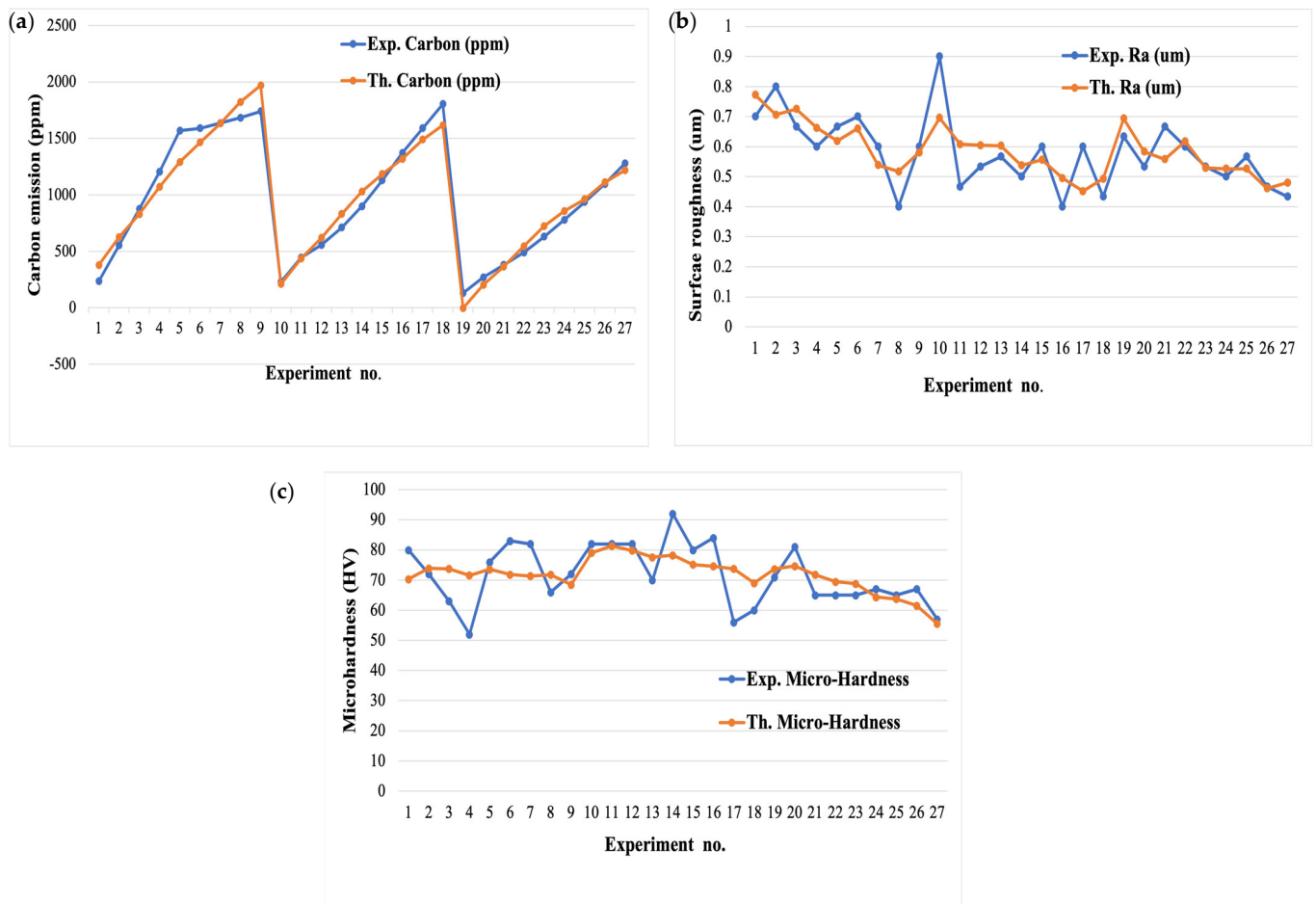


Figure 5. Percentage error between experimental and predicted values: (a) carbon emission; (b) surface roughness; (c) microhardness.

3.5. Process Optimization Using Genetic Algorithm (GA)

The genetic algorithm is a computational method that uses the concept of “survival of the fittest” among a population of solutions. The algorithm starts with a finite number of potential solutions, which are then ranked according to their fitness values and iteratively regenerated by breeding the strongest mates to produce offspring that are closer to the optimal value. To avoid convergence on local optima, population diversification is introduced through occasional mutations. This approach is more robust than traditional optimization techniques that are deterministic and prone to getting stuck at local optima [56]. Multiobjective GA is a modern method that is used to determine the optimal process control variables in real-time scenarios. This technique offers a wide range of optimal solutions, each of which is unique and nondominated. The approach provides flexibility to the machining operation by finding a set of solutions that trade off the different objectives [57]. In the current study, multiobjective optimization was performed using solver-based GA in MATLAB R2020b. The aim was to minimize carbon emission and surface roughness while maximizing the microhardness of the AZ31 alloy. The regression equations (Equations (1)–(3)) were used to write the objective function in .M file, and the GA parameters listed in Table 10 were set before running the optimization code.

Table 10. GA parameters used for process optimization.

| Setting Parameters | Value |
|---------------------------|--|
| Selection function | Tournament of size 2 |
| Crossover Function | Uniform |
| Mutation function | Gaussian |
| Direction of Migration | Forward with migration function of 0.2 |
| Distance Measure Function | Distance—Crowding |
| Population Size | 50 |
| Stopping Criteria | 100 × Number of Input Process parameters |

The boundary limits for the process variables, as given in Table 3, were used in the optimization process. The stopping criteria of 500 generations were set, and the weighted average variation in the fitness function value was observed [58]. The optimal solution was achieved in just 18 iterations, with a processing time of 1.6 s, and is listed in Table 11. To validate the GA optimization, a set of three confirmatory experimental runs were conducted using the optimal solution achieved in iteration 18 (as given in Table 11). The adequacy of the multiobjective GA was validated by performing three replicates of confirmatory tests under optimal parametric conditions. The results for carbon emission, surface roughness, and microhardness were measured and recorded in Table 12. The average percentage error between the predicted and experimental values was found to be within the acceptable range, indicating the effectiveness of the GA optimization technique.

Table 11. Process optimization results achieved from GA.

| Iteration No. | Control Parameter | | | Response Parameter | | |
|---------------|---------------------|-----------------------------|-------------------|----------------------------|--|--------------------|
| | Cutting Environment | Cutting Speed (CS) (mm/min) | Feed (F) (mm/min) | Carbon Emission (CE) (ppm) | Surface Roughness (SR) (μm) | Microhardness (HV) |
| 1 | 2.9987 | 47.1422 | 89.7649 | 0.8078 | 0.0824 | 65.4 |
| 2 | 2.9965 | 55.6425 | 89.9588 | 1.2041 | 0.1147 | 56.1 |
| 3 | 2.9965 | 48.4889 | 89.5552 | 0.8787 | 0.0872 | 64.2 |
| 4 | 2.9999 | 55.3714 | 89.8088 | 1.192 | 0.1136 | 56.4 |
| 5 | 2.9973 | 40.9588 | 89.565 | 0.4249 | 0.0623 | 71.3 |
| 6 | 2.9992 | 43.0212 | 89.7519 | 0.5627 | 0.087 | 69.3 |
| 7 | 2.9943 | 51.041 | 89.6284 | 1.0075 | 0.0966 | 61.6 |
| 8 | 2.9975 | 45.4731 | 89.3037 | 0.7076 | 0.0767 | 67.3 |
| 9 | 2.979 | 40.0061 | 75.4386 | 0.1194 | 0.0595 | 75 |
| 10 | 2.9995 | 53.65 | 89.8402 | 1.1236 | 0.1067 | 58.4 |
| 11 | 2.9997 | 41.5747 | 89.7899 | 0.4688 | 0.0642 | 70.6 |
| 12 | 2.9981 | 50.3034 | 89.7289 | 0.9718 | 0.0938 | 62.2 |
| 13 | 2.9263 | 40.0015 | 77.4545 | 0.1724 | 0.0595 | 75.7 |
| 14 | 2.991 | 53.3718 | 89.7713 | 1.1147 | 0.1056 | 58.9 |
| 15 | 2.9995 | 45.8993 | 89.8363 | 0.7383 | 0.0782 | 66.6 |
| 16 | 2.9989 | 41.1913 | 89.4703 | 0.439 | 0.063 | 71.1 |
| 17 | 2.9973 | 42.5912 | 72.1322 | 0.2346 | 0.0674 | 72.9 |
| 18 | 2.9979 | 55.9789 | 89.9804 | 1.2201 | 0.1161 | 55.7 |

Table 12. Comparison of confirmatory test and GA predicted values.

| Test No. | Control Parameter | | Constant Parameter | Response Parameter | | | |
|---------------------------------|--|-----------------------------|--------------------|---|----------------------------|--|--------------------|
| | Cutting Environment | Cutting Speed (CS) (mm/min) | | Feed (F) (mm/min) | Carbon Emission (CE) (ppm) | Surface Roughness (SR) (μm) | Microhardness (HV) |
| GA predicted values | | | | | | | |
| Iteration 18 | MQL + rice bran oil + turmeric oil + Kaolinite | 55.9789 | 89.98 | Axial depth of cut = 0.15 mm Radial depth of cut = 4 mm Tool Hang = 32 mm | 1.2201 | 0.1161 | 55.7 |
| Confirmatory test values | | | | | | | |
| 1 | MQL + rice bran oil + turmeric oil + Kaolinite | 55.9789 | 89.98 | Axial depth of cut = 0.15 mm Radial depth of cut = 4 mm Tool Hang = 32 mm | 1.2665 | 0.1323 | 57 |
| % Error | | | | | 3.6% | 12% | 2.28% |

4. Conclusions

In this research, the use of cutting fluids that are environmentally friendly was explored as a potential alternative to traditional cutting fluids in the manufacturing industry. The aim was to reduce the carbon footprint and improve the machining process when milling AZ31 magnesium alloy. Three cutting environments were studied, which included (i) dry cutting, (ii) minimum quantity lubrication (MQL) using rice bran oil as the base cutting oil and turmeric oil as an additive, and (iii) MQL using rice bran oil as the base cutting oil and turmeric oil and kaolinite nanoparticles as additives. To design the experiments, fuzzy logic was utilized, and the effects of bio-oils and kaolinite on carbon emissions, surface roughness, and microhardness were assessed. From the data analyzed, several compelling conclusions may be drawn:

- The main effects plot reveals that the third cutting environment (MQL using rice bran oil as the base cutting oil and turmeric oil and kaolinite nanoparticles as additives) yields lower levels of carbon emissions (9.21 ppm) and small surface roughness value (0.3 μm).
- Through analysis of variance (ANOVA), it is revealed that all the three input parameters, namely cutting environment, cutting speed, and feed, have a significant contribution to the reduction in carbon emission, with a percent contribution of 19.39%, 66.9%, and 7.5%, respectively.
- In the case of surface roughness according to the ANOVA, cutting speed is the most significant parameter, with a contribution of 30.10%. In addition, the cutting speed has the highest contribution of 9.8% in the case of microhardness.
- The confirmatory machining test results based on the predicted values of multiobjective genetic algorithm (GA) demonstrate that the predicted output parameter values compared to the experimental values of output parameters were within the acceptable range (errors ranging from 0% to 15%). This confirms the effectiveness and reliability of the genetic algorithm.

It is recommended that further investigations be carried out to explore the efficacy of various types of vegetable oils and nanoparticles in enhancing the machining performance and mitigating the environmental impact. The utilization of sustainable cutting fluids should be advocated in the manufacturing sector as a means of minimizing the carbon footprint.

Author Contributions: Conceptualization, S.Z., Z.A., M.K. and M.S.H.; Data curation, S.Z., M.S., S.A.K. and H.A.; Methodology, S.Z., M.K., Z.A. and M.S.H.; Analysis, S.Z., S.E. and M.R.; Software, Z.A., M.S.H. and A.H.; Validation, S.E., M.R., M.K. and A.H.; Writing—original draft M.K., S.Z., M.S., S.A.K. and H.A. All authors have read and agreed to the published version of the manuscript.

Funding: The research received no external funding.

Institutional Review Board Statement: Not applicable.

Informed Consent Statement: Not applicable.

Data Availability Statement: It will be available on request.

Conflicts of Interest: The authors declare no conflict of interest.

References

- Habib, M.S.; Sarkar, B. A Multi-Objective Approach to Sustainable Disaster Waste Management. In Proceedings of the International Conference on Industrial Engineering and Operations Management Paris, Paris, France, 26–27 July 2018; Volume 2018, pp. 1072–1083.
- Branker, K. *A Study of Energy, Carbon Dioxide Emissions and Economics in Machining: Milling and Single Point Incremental Forming*; Queen's University: Kingston, ON, Canada, 2011.
- World Resources Institute, World Greenhouse Gas Emissions: 2005. Available online: <http://www.wri.org/chart/world-greenhouse-gasemissions-2005> (accessed on 26 December 2022).
- Sun, Q.; Zhang, W. Carbon Footprint Analysis in Metal Cutting Process. In Proceedings of the International Conference on Mechanical Engineering and Material Science (MEMS), Shanghai, China, 28–30 December 2012; pp. 619–622.
- He, Y.; Liu, F.; Wu, T.; Zhong, F.P.; Peng, B. Analysis and estimation of energy consumption for numerical control machining. *Proc. Inst. Mech. Eng. Part B J. Eng. Manuf.* **2012**, *226*, 255–266. [[CrossRef](#)]
- Zhao, G.Y.; Liu, Z.Y.; He, Y.; Cao, H.J.; Guo, Y.B. Energy consumption in machining: Classification, prediction, and reduction strategy. *Energy* **2017**, *133*, 142–157. [[CrossRef](#)]
- Zhou, L.R.; Li, J.F.; Li, F.Y.; Meng, Q.; Li, J.; Xu, X.S. Energy consumption model and energy efficiency of machine tools: A comprehensive literature review. *J. Clean. Prod.* **2016**, *112*, 3721–3734. [[CrossRef](#)]
- Gajrani, K.K.; Sankar, M.R. Past and current status of eco-friendly vegetable oil based metal cutting fluids. *Mater. Today Proc.* **2017**, *4*, 3786–3795. [[CrossRef](#)]
- Zahoor, S.; Ameen, F.; Abdul-Kader, W.; Stagner, J. Environmentally conscious machining of Inconel 718: Surface roughness, tool wear, and material removal rate assessment. *Int. J. Adv. Manuf. Technol.* **2020**, *106*, 303–313. [[CrossRef](#)]
- Zahoor, S.; Abdul-Kader, W.; Ishfaq, K. Sustainability assessment of cutting fluids for flooded approach through a comparative surface integrity evaluation of IN718. *Int. J. Adv. Manuf. Technol.* **2020**, *111*, 383–395. [[CrossRef](#)]
- Prashant, D.; Kamble, C.; Waghmare, R.D.; Askhedkar, S.; Sahare, B. Multi objective optimization of turning parameters considering spindle vibration by Hybrid Taguchi Principal component analysis (HTPCA). *Mater. Today Proc.* **2017**, *4*, 2077–2084.
- Pusavec, F.; Kramar, D.; Krajnik, P.; Kopac, J. Transitioning to sustainable production—Part II: Evaluation of sustainable machining technologies. *J. Clean. Prod.* **2010**, *18*, 1211–1221. [[CrossRef](#)]
- Klocke, F.; Eisenblätter, G. Dry cutting. *CIRP Ann. Manuf. Technol.* **1997**, *46*, 519–526. [[CrossRef](#)]
- Byrne, G.; Scholta, E. Environmentally clean machining processes—A strategic approach. *CIRP Ann. Manuf. Technol.* **1993**, *42*, 471–474. [[CrossRef](#)]
- Hong, S.Y.; Zhao, Z. Thermal aspects, material considerations and cooling strategies in cryogenic machining. *Clean Technol. Environ. Policy* **1999**, *1*, 107–116. [[CrossRef](#)]
- Health and Safety Executive. COSHH Essentials for Machining with Metal Working Fluids. 2011. Available online: <http://www.hse.gov.uk/metalworking/ecoshh.htmS> (accessed on 1 December 2022).
- Hong, S.Y.; Broomer, M. Economical and ecological cryogenic machining of AISI 304 austenitic stainless steel. *Clean Technol. Environ. Policy* **2000**, *2*, 157–166. [[CrossRef](#)]
- Karadzic, I.; Masui, A.; Fujiwara, N. Purification and characterization of a protease from *Pseudomonas aeruginosa* grown in cutting oil. *J. Biosci. Bioeng.* **2004**, *98*, 145–152. [[CrossRef](#)] [[PubMed](#)]
- Mattsby-Baltzer, M.; Sandin, M.; Ahlstrom, B.; Allenmark, M.; Edebo, M.; Falsen, E.; Pedersen, K.; Rodin, N.; Thompson, R.A.; Edebo, L. Microbial growth and accumulation in industrial metal-working fluids. *Appl. Environ. Microbiol.* **1989**, *55*, 2681–2689. [[CrossRef](#)] [[PubMed](#)]
- Sutherland, J.W.; Kulur, V.N.; King, N.C.; von Turkovich, B.F. An experimental investigation of air quality in wet and dry turning. *CIRP Ann. Manuf. Technol.* **2000**, *49*, 61–64. [[CrossRef](#)]
- Gracia, U.; Ribeiro, M.V. Ti6Al4V titanium alloy end milling with minimum quantity of fluid technique use. *Mater. Manuf. Process.* **2016**, *31*, 905–918. [[CrossRef](#)]
- Liu, Z.Q.; Cai, X.J.; Chen, M.; An, Q.L. Investigation of cutting force and temperature of end-milling Ti-6Al-4V with different minimum quantity lubrication (MQL) parameters. *Proc. Inst. Mech. Eng. Part B J. Eng. Manuf.* **2011**, *225*, 1273–1279. [[CrossRef](#)]

23. Werda, S.; Duchosal, A.; Quillieca, G.L.; Morandea, A.; Leroya, R. Minimum quantity lubrication: Influence of the oil nature on surface integrity. *Procedia CIRP* **2016**, *45*, 287–290. [CrossRef]
24. Sevim, Z.; Erhan, S.A. Lubricant base stocks from vegetable oils. *Ind. Crops Prod.* **2000**, *11*, 277–282.
25. Campanella, A.; Rustoy, E.; Baldessari, A.; Baltanas, M.A. Lubricants from chemically modified vegetable oils. *Bioresour. Technol.* **2010**, *101*, 245–254. [CrossRef]
26. Jayadas, N.H.; Nair, K.P. Coconut oil as base oil for industrial lubricants—Evaluation and modification of thermal, oxidative and low temperature properties. *Tribol. Int.* **2006**, *39*, 873–878. [CrossRef]
27. Peng, J.; Gao, W.; Gupta, B.K.; Liu, Z.; Romero-Aburto, R.; Ge, L.; Ajayan, P.M. Graphene quantum dots derived from carbon fibers. *Nano Lett.* **2012**, *12*, 844–849. [CrossRef] [PubMed]
28. Rani, S.; Joy, M.L.; Nair, K.P. Evaluation of physio chemical and tribological properties of rice bran oil—Biodegradable and potential base stock for industrial lubricants. *Ind. Crops Prod.* **2015**, *65*, 328–333. [CrossRef]
29. Talib, N.; Rahim, E.A. Performance of modified jatropha oil in combination with hexagonal boron nitride particles as a bio-based lubricant for green machining. *Tribol. Int.* **2018**, *118*, 89–104. [CrossRef]
30. da Silva, P.M.; Gauche, C.; Gonzaga, L.V.; Costa, A.C.O.; Fett, R. Honey: Chemical composition, stability and authenticity. *Food Chem.* **2016**, *196*, 309–323. [CrossRef] [PubMed]
31. Xiao, Y.; Zhao, R.; Yan, W.; Zhu, X. Analysis and Evaluation of Energy Consumption and Carbon Emission Levels of Products Produced by Different Kinds of Equipment Based on Green Development Concept. *Sustainability* **2022**, *14*, 7631. [CrossRef]
32. Anwar, F.; Hussain, A.I.; Iqbal, S.; Bhangar, M.I. Enhancement of the oxidative stability of some vegetable oils by blending with moringa oleifera oil. *Food Chem.* **2007**, *103*, 1181–1191. [CrossRef]
33. Selvam, R.; Subramanian, L.; Gayathri, R.; Angayarkanni, N. The anti-oxidant activity of turmeric (*Curcuma longa*). *J. Ethnopharmacol.* **1995**, *47*, 59–67. [CrossRef]
34. Peña-Parás, L.; Taha-Tijerina, J.; García, A.; Maldonado, D.; González, J.A.; Molina, D.; Cantú, P. Antiwear and extreme pressure properties of nanofluids for industrial applications. *Tribol. Trans.* **2014**, *57*, 1072–1076. [CrossRef]
35. Xu, Z.Y.; Xu, Y.; Hu, K.H.; Xu, Y.F.; Hu, X.G. Formation and tribological properties of hollow sphere-like nano-MoS₂ precipitated in TiO₂ particles. *Tribol. Int.* **2015**, *81*, 139–148. [CrossRef]
36. Alves, S.M.; Barros, B.S.; Trajano, M.F.; Ribeiro, K.S.B.; Moura, E.J.T.I. Tribological behavior of vegetable oil-based lubricants with nano particles of oxides in boundary lubrication conditions. *Tribol. Int.* **2013**, *65*, 28–36. [CrossRef]
37. Vergaro, V.; Abdullayev, E.; Lvov, Y.M.; Zeitoun, A.; Cingolani, R.; Rinaldi, R.; Leporatti, S. Cytocompatibility and uptake of halloysite clay nano tubes. *Biomacromolecules* **2010**, *11*, 820–826. [CrossRef] [PubMed]
38. Shchukin, D.G.; Sukhorukov, G.B.; Price, R.R.; Lvov, Y.M. Halloysite nanotubes as biomimetic nanoreactors. *Small* **2005**, *1*, 510–513. [CrossRef] [PubMed]
39. White, R.D.; Bavykin, D.V.; Walsh, F.C. The stability of halloysite nanotubes in acidic and alkaline aqueous suspensions. *Nanotechnology* **2012**, *23*, 065705. [CrossRef] [PubMed]
40. Shamsi, M.H.; Geckeler, K.E. The first biopolymer wrapped non-carbon nanotubes. *Nanotechnology* **2008**, *19*, 075604. [CrossRef] [PubMed]
41. Spectral Evolution. (n.d.). Distinguish Kaolinite from Halloysite. Available online: <https://spectralevolution.com/applications/mining/distinguish-kaolinite-from-halloysite/#:~:text=Kaolinite%20and%20halloysite%20are%20both> (accessed on 1 December 2022).
42. Bourdelle, F.; Dubois, M.; Lloret, E.; Durand, C.; Addad, A.; Bounoua, S.; Ventalon, S.; Recourt, P. Kaolinite-to-Chlorite Conversion from Si,Al-Rich Fluid-Origin Veins/Fe-Rich Carboniferous Shale Interaction. *Minerals* **2021**, *11*, 804. [CrossRef]
43. Du, X.; Pang, D.; Zhao, Y.; Hou, Z.; Wang, H.; Cheng, Y. Investigation into the adsorption of CO₂, N₂ and CH₄ on kaolinite clay. *Arab. J. Chem.* **2022**, *15*, 103665. [CrossRef]
44. McDonough, W.F. The composition of the Earth. *Int. Geophys.* **2001**, *76*, 3–23.
45. Gray, J.E.; Luan, B. Protective coatings on magnesium and its alloys, a critical review. *J. Alloys Compd.* **2002**, *336*, 88–113. [CrossRef]
46. Hombeger, H.; Virtanen, S.; Boccaccini, R. Biomedical coating on magnesium alloys—a review. *Acta Biomater* **2012**, *8*, 2442–2455.
47. Shetty, R.; Hegde, A. Taguchi based fuzzy logic model for optimisation and prediction of surface roughness during AWJM of DRCUFP composites. *Manuf. Rev.* **2022**, *9*, 1–15. [CrossRef]
48. Muhammad, R. A Fuzzy Logic Model for the Analysis of Ultrasonic Vibration Assisted Turning and Conventional Turning of Ti-Based Alloy. *Materials* **2021**, *14*, 6572. [CrossRef] [PubMed]
49. Available online: <https://www.en-standard.eu/bs-en-50543-2011-electronic-portable-and-transportable-apparatus-designed-to-detect-and-measure-carbon-dioxide-and-or-carbon-monoxide-in-indoor-ambient-air-requirements-and-test-methods/> (accessed on 1 December 2022).
50. Puls, H.; Klocke, F.; Lung, D. Experimental investigation on friction under metal cutting conditions. *Wear* **2014**, *310*, 63–71. [CrossRef]
51. Kumar, M.P.; Amarnath, K.; Kumar, M.S. A review on heat generation in metal cutting. *Int. J. Eng. Manag. Res. IJEMR* **2015**, *5*, 193–197.
52. Zhao, J.; Liu, Z.; Wang, B.; Hu, J.; Wan, Y. Tool coating effects on cutting temperature during metal cutting processes: Comprehensive review and future research directions. *Mech. Syst. Signal Process.* **2021**, *150*, 107302. [CrossRef]

53. Zahoor, S.; Saleem, M.Q.; Abdul-Kader, W.; Ishfaq, K.; Shehzad, A.; Ghani, H.U.; Hussain, A.; Usman, M.; Dawood, M. Improving surface integrity aspects of AISI 316L in the context of bioimplant applications. *Int. J. Adv. Manuf. Technol.* **2019**, *105*, 2857–2867. [[CrossRef](#)]
54. Zahoor, S.; Mufti, N.A.; Saleem, M.Q.; Shehzad, A. An investigation into surface integrity of AISI P20 machined under the influence of spindle forced vibration. *Int. J. Adv. Manuf. Technol.* **2018**, *96*, 3565–3574. [[CrossRef](#)]
55. Zahoor, S.; Mufti, N.A.; Saleem, M.Q.; Mughal, M.P.; Qureshi, M.A.M. Effect of machine tool's spindle forced vibrations on surface roughness, dimensional accuracy and tool wear in vertical milling of AISI P20. *Int. J. Adv. Manuf. Technol.* **2017**, *89*, 3671–3679. [[CrossRef](#)]
56. Biswas, M.S.; Mandal, K.; Sarkar, S. MOGA approach in WEDM of advanced aluminium alloy. *Mater. Today Proc.* **2020**, *26*, 887–890. [[CrossRef](#)]
57. Han, X.; Zhang, Z. Topological optimization of phononic crystal thin plate by a Genetic Algorithm. *Sci. Rep.* **2019**, *9*, 8331. [[CrossRef](#)]
58. Zahoor, S.; Azam, H.A.; Mughal, M.P.; Ahmed, N.; Rehman, M.; Hussain, A. WEDM of complex profile of IN718: Multi-objective GA-based optimization of surface roughness, dimensional deviation, and cutting speed. *Int. J. Adv. Manuf. Technol.* **2021**, *14*, 2289–2307. [[CrossRef](#)]

Disclaimer/Publisher's Note: The statements, opinions and data contained in all publications are solely those of the individual author(s) and contributor(s) and not of MDPI and/or the editor(s). MDPI and/or the editor(s) disclaim responsibility for any injury to people or property resulting from any ideas, methods, instructions or products referred to in the content.